vol. 43, n.° 1, enero-abril de 2021
ISSN impreso: 0120-0283 • ISSN en línea: 2145-8553

The carbonate platform of the Upper Tibasosa Formation, Lower Cretaceous, Eastern Cordillera Basin, Firavitoba-Boyacá, Colombia

Juan Sebastián Gómez-Neita[1,2*]; Pedro Augusto Santos da Silva[2]; Laura Estefania Garzón-Rojas[1,2]; Luz Angie Patiño-Ballesteros[1]; Laura Alexandra Barrantes[1]; Anna Andressa Evangelista-Nogueira[2]

How to cite: Gómez-Neita, J.S.; Santos da Silva, P.A.; Garzón-Rojas, L.E.; Patiño-Ballesteros, L.A.; Barrantes, L.A.; Evangelista-Nogueira, A.A. (2021). The carbonate platform of the Upper Tibasosa Formation, Lower Cretaceous, Eastern Cordillera Basin, Firavitoba-Boyacá, Colombia. *Boletín de Geología, 43*(1), 15-33. https://doi.org/10.18273/revbol.v43n1-2021001

Abstract

The Tibasosa Formation is the main source of limestones in Boyacá. This unit corresponds to a Valanginian-Albian age according to the fossil content in the Eastern Cordillera Basin, recording the first incursion of the Cretaceous sea in Firavitoba. Outcrop-based facies and stratigraphic analyzes of the ~12 m-thick siliciclastic-carbonate succession of the uppermost Tibasosa Formation indicate tidal and carbonate systems. Ten facies/microfacies are grouped into two facies associations (FAs): FA1, tidal flat deposits consist of laminated sandstones/siltstones and floatstones with a single organism dominance (bivalve shells); and FA2 comprises fossiliferous rudstones, floatstones, packstones, and wackstones, representing a carbonate platform. The petrographic description determined rock textures/genesis and the diagenetic sequence with features of the eodiagenesis, mesodiagenesis, and telodiagenesis suggesting a primary origin of these carbonates. The analysis using cathodoluminescence (CL), energy disperse spectrometry (EDS), and scanning electron microscopy (SEM) allowed identify compositional differences, cementation phases, and morphological features in different processes as micritization, neomorphism, porosity, pyritization, compaction, cementation, fracturing, and weathering. The interpretation of facies and microfacies indicated a deposition mainly in a shallow platform with variation in the hydraulic conditions, warm waters, and episodic events of storms/tsunamis that fragmented the bioclasts. A shallow marine system in the Eastern Cordillera Basin during Cretaceous indicates a large transgressive event that flooded hundreds of kilometers, being a link with the Pacific Ocean before the Andes uplift. The main diagenetic events correspond to micritization, cementation of calcite, and mechanical/chemical compaction as a result of microbial activity, dissolution, precipitation in the vadose/phreatic zone, and burial diagenesis. The diagenetic sequence events reveal the incidence of marine and meteoric process that reduced porosity and attest to the microbial activity in carbonate precipitated. This new interpretation allows the understanding of carbonate platforms in the Eastern Cordillera Basin for future correlations of the Cretaceous sea in Colombia.

Keywords: Limestones; Diagenesis; Eastern Cordillera Basin; Upper Tibasosa Formation; Cathodoluminescence (CL).

La plataforma carbonática de la Formación Tibasosa Superior, Cretáceo Inferior, Cuenca Cordillera Oriental, Firavitoba-Boyacá, Colombia

Resumen

La Formación Tibasosa es la principal fuente de calizas en Boyacá. Esta unidad se depositó entre el Valanginiano-Albiano según el contenido fósil en la Cuenca Cordillera Oriental, registrando la primera incursión del mar Cretácico en Firavitoba. Los análisis de facies y estratigráficos de una sucesión carbonática-siliciclástica de ~12 m de espesor de la Formación Tibasosa Superior indican sistemas mareales/carbonáticos. Diez facies/microfacies se agruparon en dos asociaciones de facies (AFs): AF1, planicie mareal consiste en areniscas/limolitas laminadas y *floatstones* con un solo tipo de organismo dominante (conchas de bivalvos); y AF2 comprende *rudstones*, *floatstones*, *packstones* y *wackstones*, representando una plataforma carbonática. La descripción petrográfica determinó la textura/génesis y la secuencia diagenética con características de la eodiagénesis, mesodiagénesis y telodiagénesis sugiriendo un origen primario de estos carbonatos. El análisis mediante catodoluminiscencia (CL), espectrometría de energía dispersa (EDS) y microscopía electrónica de barrido (MEB) permitió identificar diferencias composicionales, fases de cementación y características morfológicas en diferentes procesos como micritización, neomorfismo, porosidad, piritización, compactación, cementación, fracturamiento. y meteorización. La interpretación de facies/microfacies indicó una deposición en una plataforma poco profunda con condiciones hidráulicas fluctuantes, aguas cálidas y eventos de tormentas/tsunamis que fragmentaron los bioclastos. Este sistema deposicional en la Cuenca Cordillera Oriental durante el Cretácico indica un gran evento transgresivo que inundó cientos de kilómetros, revelando conexión con el Océano Pacífico antes del levantamiento Andino. Los principales eventos diagenéticos corresponden a la micritización, cementación de calcita y compactación mecánica/química como resultado de la actividad microbiana, disolución, precipitación en la zona vadosa/freática y diagénesis de enterramiento. La secuencia diagenética revela la incidencia de procesos marinos y meteóricos que redujeron la porosidad y corroboran la actividad microbiana en el carbonato precipitado. Esta nueva interpretación permite comprender las plataformas carbonatadas en la Cuenca Cordillera Oriental para futuras correlaciones del mar Cretácico en Colombia.

Palabras clave: Calizas; Diagénesis; Cuenca Cordillera Oriental; Formación Tibasosa Superior; Catodoluminiscencia (CL).

[1]Grupo de Investigación en Ingeniería Geológica, Universidad Pedagógica y Tecnológica de Colombia, Sogamoso, Colombia. (*) juan.gomezneita@uptc.edu.co; laura.garzon01@uptc.edu.co; luz.patino01@uptc.edu.co; laura.barrantes@uptc.edu.co
[2]Grupo de Análise de Bacias Sedimentares da Amazônia (GSED), Universidade Federal do Pará, Belém, Brasil. pedrogeologia8@hotmail.com; aenogueira@ufpa.br

Introduction

Two parameters control the limestones features, the nature of the carbonate fabric associated to depositional environments, water chemistry, and biologic action; and the diagenetic processes which affect the sediments according to the type of original material, temperature, depth, fluids, and tectonics; generating changes in texture, porosity, mineralogy, and chemistry (Boggs Jr., 2006; da Silva, 2019). Changes in carbonate sediments occur in three diagenetic realms: marine, meteoric and burial with high potential of diagenesis mainly due to the abundance of aragonite-calcite which could supply $CaCO_3$ for cement in tropical calcareous deposits in the meteoric environment (*i.e.*, diagenetic alteration; James and Coquette, 1990; Seibel and James, 2017; Li *et al.*, 2018), as is the case of Mesozoic limestones from Colombia which correspond to the rocks of Upper Tibasosa Formation in the Eastern Cordillera Basin, in the state of Boyacá.

During the Cretaceous, the Eastern Cordillera Basin in Colombia records an important phase of marine deposition due to the geographic location and a rise in the sea level. Renzoni (1981) defined the basal unit of the Cretaceous in the region of Sogamoso Valley as Tibasosa Formation, which is composed mainly of sandstones, siltstones, marls and many beds of limestones in the Upper Member, with a systematic thinning-northward, towards to the Floresta massif. However, Reyes (1984) proposed the formulation of a new unit denominated as Belencito Formation that corresponds to the Upper Calcareous Member of Renzoni (1981), due to the economic importance of these rocks in the region. The geological charts of Sogamoso-Paz de Rio and Duitama define this calcareous member as Upper Tibasosa Formation that will use in this work (Ulloa *et al.*, 1998a; Renzoni and Rosas, 1967).

The Upper Tibasosa Formation has carbonates with diagenetic evidence such as micritization, compaction (*i.e.*, mechanical and chemical), pyritization, dissolution, recrystallization, cementation (*e.g.*, calcite and silica) and fracturing (Morad *et al.*, 2019), which indicate a primary origin of the calcareous sediments subsequently affected by the lithification. All these features are common in the Upper Tibasosa Formation rocks, representing an important record of shallow-water limestones in the State of Boyacá and strong evidence of the Cretaceous sea in Colombia during this period. This study aims to define the depositional environments of these calcareous rocks, according to facies and microfacies description, and identify the main diagenetic processes in their respective phases (*i.e.*, eodiagenesis, mesodiagenesis, and telodiagenesis). In this sense, the lithostratigraphic analysis contributes to the correlation of the Tibasosa Formation with other Early Cretaceous carbonate rocks in Colombia affected by a main transgressive event.

Geological setting

The Eastern Cordillera Basin extends across the states of Cundinamarca, Boyacá, Santander, Norte de Santander and some areas in Huila, Tolima, Cesar, Guajira, Caquetá, Meta, Casanare, and Arauca, it is limited to the north by the Santander High, to the east by the inverse fault system of the Eastern Cordillera, to the south by the Algeciras-Garzon fault system and the west by the Bituima and Salina faults (Quintero *et al.*, 2014). The Basin development began during the Triassic with a syn-rift mega sequence due to the separation of North and South America, later a back-arc basin (Early Cretaceous-Campanian) was formed and finally with the accretion of the Western Cordillera was developed a pre-foreland basin (Upper Mashtrictian-Paleocene); after this event the Eastern Cordillera Basin faced two deformation phases, the first one associated to the loading effects during the Eocene and the second one to the Andean uplift (Miocene), generating the formation of the current geomorphological setting of the Eastern Cordillera and separating the Valle Medio and Llanos basins (Cooper *et al.*, 1995).

The first sequence (*i.e.*, the syn-rift event) is exposed in the Eastern Cordillera with variable thicknesses due to the extension of faults that controlled the deposition (Cediel, 1968), the continental facies associated with the Jurassic and early basal Cretaceous deposits changed to shallow marine deposits in the transition between the Berriasian to Valanginian (Cooper *et al.*, 1995), in a basin with an approximate extension of 180 km divided by the Santander Floresta horst located to the northeast of the study area (Sarmiento-Rojas *et al.*, 2006). Rocks of the Tibasosa Formation, at least locally in the Sogamoso, Duitama, and Belen towns, rest with angular unconformity-nonconformity on Early Mesozoic (*e.g.*, Giron Formation), Paleozoic (*e.g.*, Cuche Formation) and crystalline rocks (*e.g.*, Cuarcites of the metamorphic complex; Reyes, 1984; Sarmiento-Rojas *et al.*, 2006); in the same way exist faulted contacts between the Upper Tibasosa Formation with Cenozoic units caused by the action

of the Soapaga fault located about 2 km from the study area (Figure 1). This structure is an inverted fault (Julivert, 1970) with SW-NE direction forming important areas of folded limestones, partially covered by the quaternary alluvial deposits (Miranda and Niño, 2016).

The Tibasosa Formation is the basal unit of the Cretaceous in the area of Firavitoba, this unit corresponds to a Valanginian to Albian age, according to the fossil content (Reyes, 1984; Patarroyo, 2002; Patarroyo *et al.*, 2014). The stratigraphic sequence evidence about the first incursion of the Cretaceous sea in the Eastern Cordillera Basin, being concordant with the occurrence of the Rosablanca and Paja formations in the west of the Boyacá state with minor chronological variations (Rojas and Sandy, 2019). The Tibasosa Formation comprises of four members according to Renzoni (1981), the Lower Member formed by conglomerates, sandstones, and siltstones, the Lower Calcareous Member with marls and limestones, the Intermediate Sandstone Member and the Upper Calcareous Member formed by biomicrites, biosparites, and black shales (Reyes, 1984; Patarroyo *et al.*, 2014).

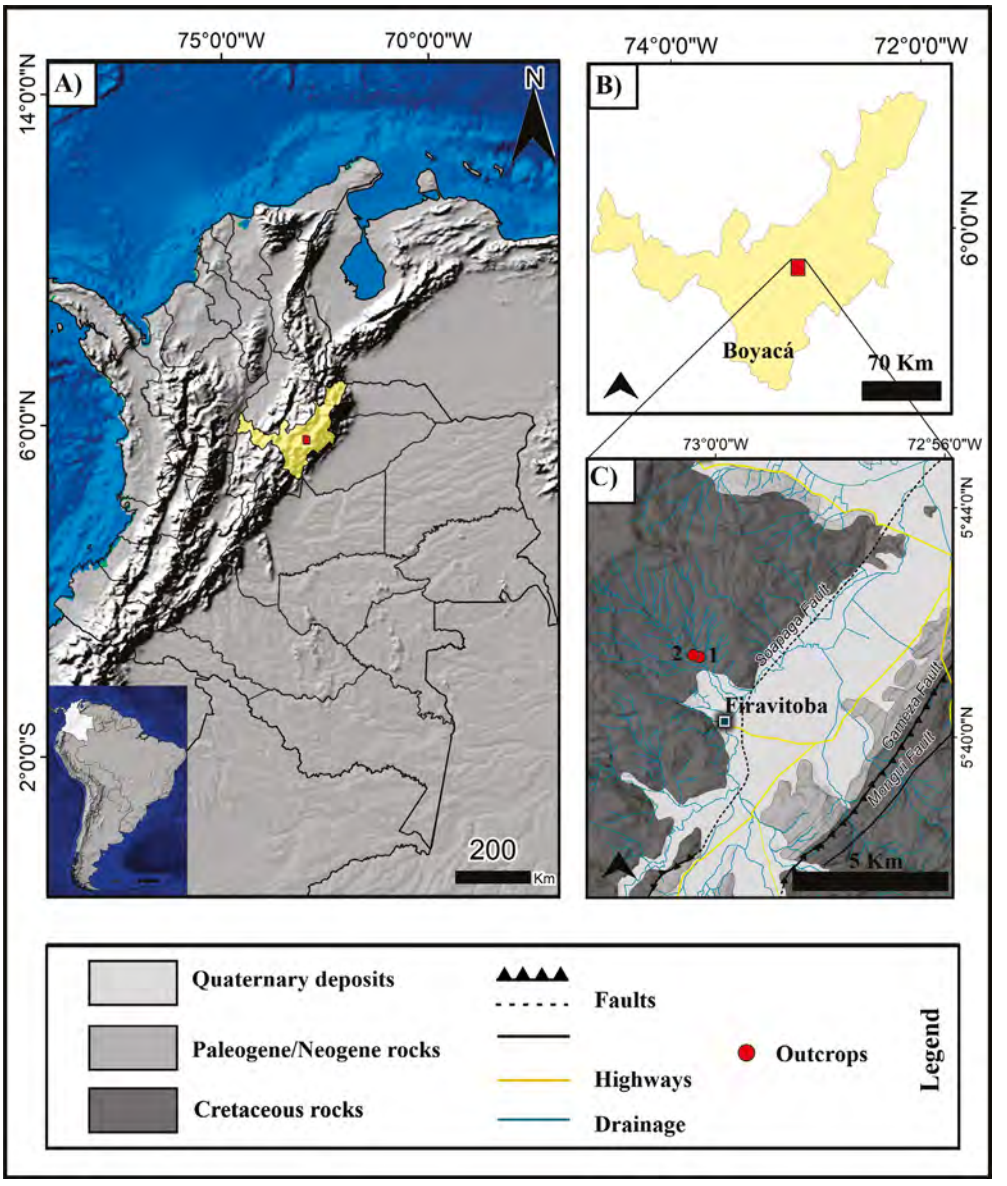

Figure 1. Location map of the study area. **A.** Location of Colombia in South America. **B.** The state of Boyacá highlighting the study area. **C.** Geological map positioning the outcrops of this study. Modified of Renzoni *et al.* (1998), Ulloa *et al.* (1998a, 1998b), and Renzoni and Rosas (1967).

The Firavitoba city registers the entire sequence of the Upper Calcareous Member where there are approximately ten beds of limestones interbedded with marls, shales, and sandstones. According to the description by Miranda and Niño (2016) for *Central de Triturados Ltda* Company, these beds are composed mainly by biomicrites, wackstones and packstones with a variable content of $CaCO_3$, detrital material (quartz) and iron oxides/hydroxides what makes these an important focus of study for the cement industry. This unit has been interpreted as marine deposits due to the fossil content (Reyes, 1984), however, it still necessary detailed studies of facies/microfacies to define more precisely the depositional environment and the main diagenetic features in these limestones.

Methodology

The analyzes include 20 samples of limestones from two outcrops in the city of Firavitoba, Boyacá in Colombia (Figure 2). The facies description follows the methodology of Walker and James (1992) emphasizing bed geometry, granulometry (bioclast and grain size), mineralogical composition, sorting, fossil content, and bioturbation to identify sedimentary processes associated with specific depositional systems.

The preparation of 20 thin sections carried out at the Universidad Pedagógica y Tecnológica de Colombia, in an attempt to define the limestone components (allochems, micrite, terrigenous grains, cement, and pores) by counting of 300 points to determine microfacies according to the Classification of Dunham (1962) modified by Embry and Klovan (1971). Additional tests as scanning electron microscopy (SEM), energy disperse spectroscopy (EDS), and cathodoluminescence (CL) established minerals, textures, semi-quantitative chemical composition, and cementation phases. SEM analysis carried out at the laboratory of microanalysis of the Geoscience Institute of UFPA-Brazil; after coating with a thin layer of gold, the samples were analyzed using backscattered electron (BSE) and secondary electron (SE) imaging under accelerating voltage of 20 kV, the working distance of 15 mm and an increase of approximately 200x in the microanalyzer LEO 1430. The CL tests allowed to determine information about mineral phases and cementation to define different compositions, the operating voltage was 10-15 kV with a beam current of 150-250 μA and exposition time of 10-30 seconds in a petrographic microscope Leica DM 4500 P LED coupled with Optical Cathodoluminescence CL 8200 MKS5-2 on the cathodoluminescence laboratory of UFPA-Brazil (LCL-UFPA).

Results

Facies description and paleoenvironmental interpretation

Were described two outcrops (Figure 2) in the municipality of Firavitoba, Boyacá, in the area of Loma Redonda next to the Mombita drainage, the identification of Tibasosa Superior Formation was defined according to the lithology, geomorphology, sedimentary structures, and characteristic fossil content. The outcrops consist mainly of carbonate rocks with few siliciclastic contributions in folded beds with a strike of N84°W dipping 9°NE next to the Soapaga fault.

Ten facies/microfacies were described (Table 1) and grouped in two FAs: mixed tidal flat (FA1) and carbonate platform (FA2) defined mainly according to the proportion of detrital and carbonate components, sedimentary structures, and fossils. The FA1 - mixed tidal flat, consisting of the facies and microfacies: massive sandstone (Sm), laminated siltstone (Sl), massive mudstone (Mm), and bioclastic floatstone (occasionally with a high content of fragmented bivalves) (Fb). The FA2 - shallow platform deposits, consisting of the facies and microfacies: massive lime-mudstone (Lm), bioclastic wackestone (Wb), bioclastic wackestone with terrigenous grains (Wbt), bioclastic packstone (Pb), bioclastic packstone with terrigenous grains (Pbt), bioclastic floatstone (Fb) and bioclastic rudstone (Rb) associated to the high biological activity of invertebrate fauna as bivalves, gastropods, echinoderms, foraminifera, and ostracods.

The Sm facies presents layers <10 cm with a pale-yellow color, the grain size corresponds to medium sand composed mainly by monocrystalline quartz and fragments of muddy rocks, cemented by silica, calcite and iron oxides (Figure 3A); the grains present subangular to subrounded shapes with medium sphericity and sharps contacts with the Fb facies. The Sl facies consists of pale gray layers of about 20 cm composed of quartz, clay minerals and organic matter with a plane/wavy lamination, commonly associated with the Mm, Fb, and Pb facies showing net contacts. The Mm facies is associated with Sl and Fb facies, it has a pale yellow color with a thickness of 20-25 cm; the composition corresponds to clay minerals, organic

matter, and rare quartz grains, exhibiting graded to net contacts. The Lm microfacies has a medium gray color; it comprises of micrite (90-92%), grains of monocrystalline quartz (4%), organic matter (2%), and fragmented/entire bivalve bioclasts (2%); it is associated with Fb microfacies presenting net contacts.

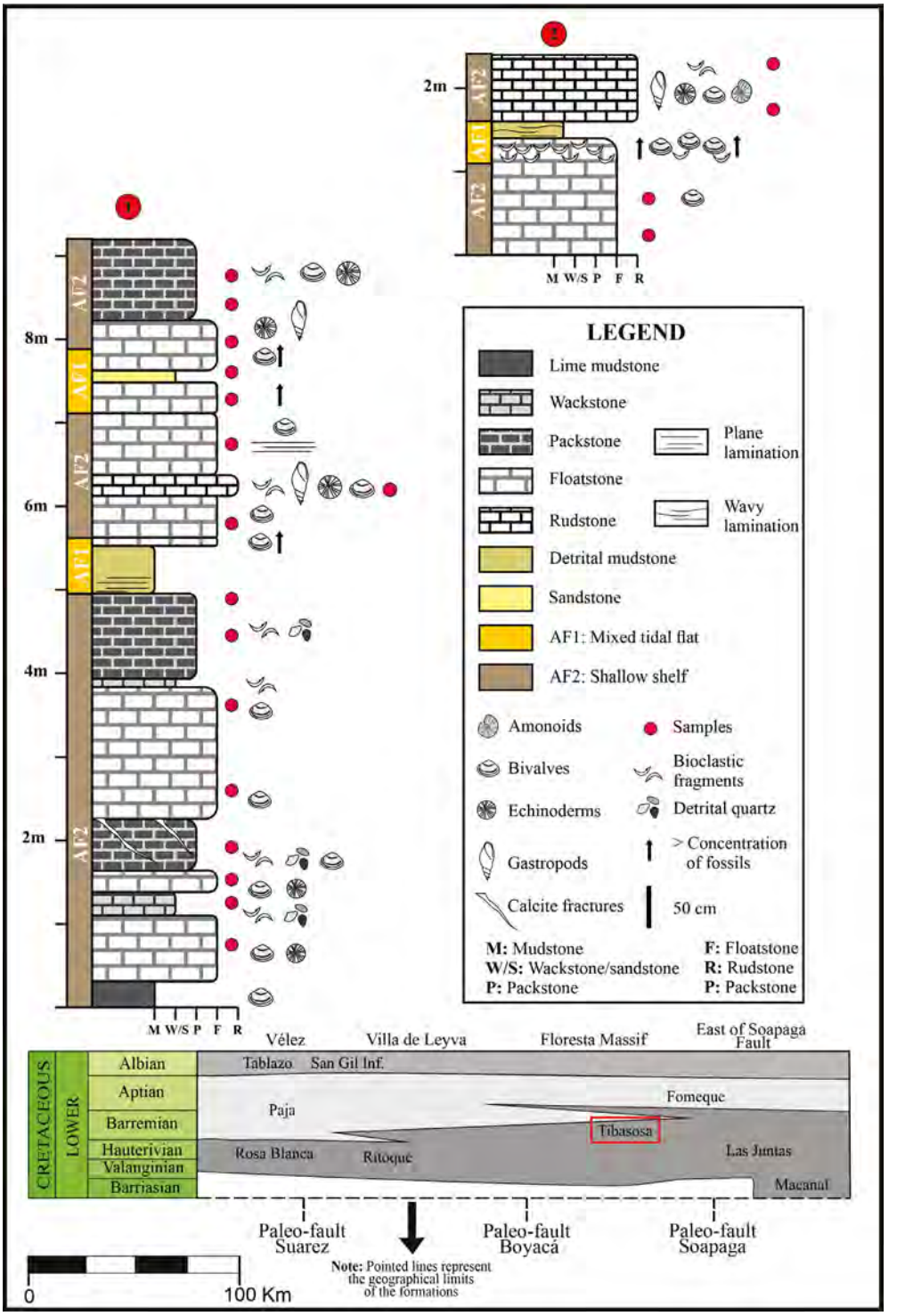

Figure 2. Outcrops for the Upper Tibasosa Formation in the area of Loma Redonda, Firavitoba-Boyacá, Colombia. The location of outcrops is indicated in Figure 1, stratigraphic chart extracted of Sarmiento-Rojas *et al*. (2006).

Table 1. Facies/microfacies of the Upper Tibasosa Formation with nomenclature, descriptions, and processes.

Name	Facies	Description	Process
Sm	Massive sandstone	Medium sandstone with quartz grains and calcite cement	Rapid deposition (or liquefaction) and carbonate cementation obliterating the original structure (associated with chemical precipitation and percolation of fluids during diagenesis)
Sl	Laminated siltstone	Quartz siltstones with plane to wavy laminations	Alternating traction currents and suspension in oscillating currents
Mm	Massive mudstone	Massive mudstone composed of quartz (rare), organic matter, and clay minerals	Deposition by decantation in low energy conditions, liquefaction in water-saturated environments
Lm	Massive lime mudstone	Massive mudstone with entire bivalves in proportions <10%	Biochemical precipitation in low energy conditions associated to organic activity
Fb	Bioclastic floatstone	Massive floatstone with occasional oriented and fragmented bioclasts. Concave-convex up stacking of bioclasts	Biochemical precipitation, preservation of bioclast larger than 2 mm. Orientation and fragmentation associated with episodic storms/tsunamis events
Wb	Bioclastic wackestone	Massive with fragmented bioclasts	Biochemical precipitation and preservation of bioclasts in addition to diagenetic processes
Wbt	Bioclastic wackestone with terrigenous grains	Massive wackestone with bioclasts and quartz grains in a micritic matrix	Biochemical precipitation, preservation of bioclasts and influx of terrigenous grains by traction currents
Pb	Bioclastic packstone	Massive with fragmented bioclasts and punctual to tangential contacts	Biochemical precipitation and preservation of bioclasts
Pbt	Bioclastic packstone with terrigenous grains	Massive packstone with bioclasts and quartz grains, with an early and late phase of silica cementation	Biochemical precipitation and preservation of bioclasts cemented and silicified associated with silica precipitation and quartz dissolution, terrigenous grains by traction currents
Rb	Bioclastic rudstone	Massive with entire fossils >2 mm in a wackestone matrix	Biochemical precipitation in low energy conditions, preservation of different bioclasts as bivalves, gastropods and echinoderms

The microfacies Fb is medium gray, it is the most abundant microfacies in the sedimentary succession, formed by micrite (68%), fragmented/entire bioclasts of bivalves, echinoids (Figure 3D), gastropods, and subordinated foraminifera and ammonoids replaced commonly by sparite (26%), and quartz (6%) (Figure 3C), sporadically with oriented and fragmented shells forming a representative bed (Figure 3B), associated with Sm, Sl, Mm, Lm, Wb, Wbt, Pb, Pbt, and Rb facies presenting net and graded contacts.

The Wb microfacies has a medium gray color, massive texture, and evidence of fractures. It consists of micrite (61%), fragments of bivalves, gastropods, foraminifera, algae, and ostracods (34%); organic matter (2%), iron oxides (3%) and rare quartz grains; it is associated with Fb and Pbt facies showing net contacts. The Wbt facies presents a similar composition to the Wb facies (*e.g.*, the same color and allochems), however, with a high proportion of terrigenous grains represented mainly of quartz (~10%) (Figure 3F); it is associated with Fb facies exhibiting sharp contacts.

The Pb microfacies is gray, massive, and has micrite matrix (28%), fragments of bivalves, gastropods, and echinoids (57%) (Figure 3E), iron oxides and hydroxide (7%), quartz (5%), and glauconite (Tr); it is related with the Fb facies presenting sharp contacts. The microfacies Pbt is similar to the Pb facies (*e.g.*, same color), it comprises of peloids, fragments of bivalves, and echinoids (40%), grains of monocrystalline quartz (32%), micrite (22%) and iron oxides/hydroxides (6%); it is related with Fb facies presenting sharp contacts. The Rb microfacies has a light gray color, and it is formed mainly by entire/fragmented bioclasts of bivalves, gastropods and echinoids (62%), micrite (32%), iron oxides (4%) and quartz (2%); it is associated with Fb and Sl facies showing net to graded contacts.

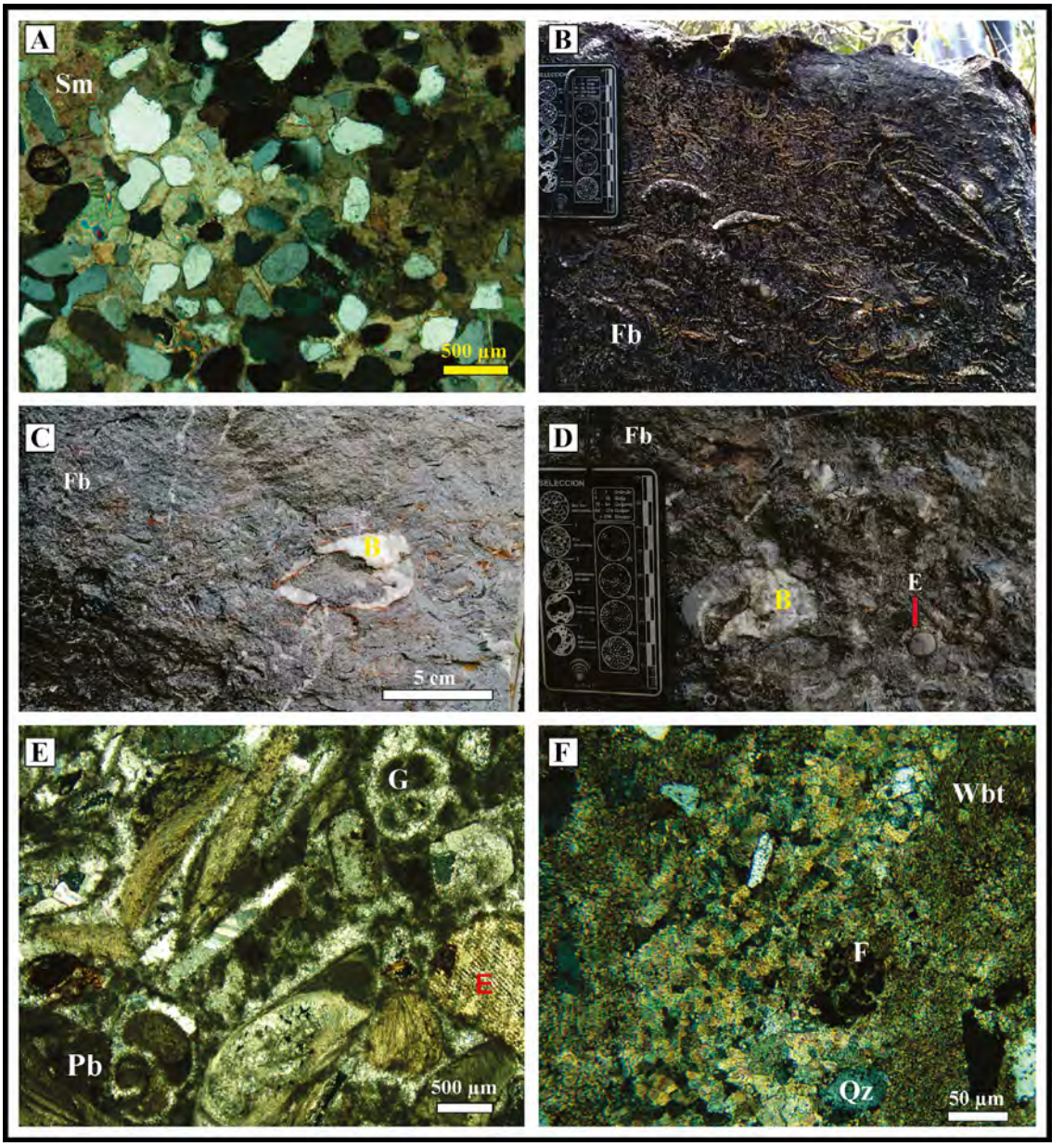

Figure 3. Facies and microfacies of the Upper Tibasosa Formation in the area of Loma Redonda, Firavitoba-Boyacá, Colombia. **A.** Facies massive sandstone with calcite cement. **B.** Microfacies bioclastic floatstone with a high concentration of oriented and fragmented bivalve shells. **C.** Microfacies bioclastic floatstone with bivalves replaced by sparry. **D.** Microfacies bioclastic floatstone with bivalves and echinoderms. **E.** Microfacies bioclastic packstone with gastropods, echinoderms, and fragments of bivalves, micrite matrix and sparry cement. **F.** Microfacies bioclastic wackestone with terrigenous grains. B: bivalve, E: echinoderm, F: foraminifer, Pb: bioclastic packstone, G: gastropod, Qz: quartz.

The FA1 represents the accumulation of detrital and carbonate rocks. Probably, in this setting, lagoons formed due to the tidal influence that allowed the accumulation of thick deposits of marls and mudstones with high organic matter content described in other outcrops of the Upper Tibasosa Formation in Boyacá (Reyes, 1984; Miranda and Niño, 2016). Moreover, the dominance of a single kind of organism (*i.e.*, low diversity, in this case, bivalve shells) in a high proportion is an excellent indicator of restricted environments with an influx of terrigenous grains. FA2 reflects a shallow carbonate platform deposited in the euphotic zone due to the presence of micrite, horizontal shape of beds and absence of large quantities of foraminifera and red algae which found in steepened ramps in the oligophotic framework (Pomar, 2001). The predominance of micrite, few contents of terrigenous grains and diversity of marine invertebrates suggest a shallow water environment (Tucker and Wright, 1990; Kiessling *et al.*, 2003; da Silva, 2019).

Diagenesis

The term diagenesis describes the physicochemical changes of sediments after deposition in temperatures and depths below about 250°C and 5000 m (James and Coquette, 1990; Milliken, 2003; Nichols, 2009). The geological history of the Tibasosa Formation suggests the three major phases of diagenesis, reflecting the syngenetic, mesogenetic, and telogenetic alterations in the studied stratigraphic section (Scholle and Ulmer-Scholle, 2003). In carbonate sediments, diagenesis includes cementation, porosity generation, changes in trace elements, and isotopic signature (Tucker and Wright, 1990; Moore and Wade, 2013). The Upper Tibasosa Formation limestones exhibits evidence of micritization, cementation, mechanical/chemical compaction, silicification, pyritization, changes in porosity, neomorphism, and fracturing; recognized with petrographic and chemical analyzes allowing the construction of the diagenetic sequence.

Micritization. This process forms dark envelopes on bioclast carapaces (Figures 4A, 4B), and is frequent in the microfacies Wb, Wbt, Pb, Pbt, Fb, and Rb. It represents the bacterial/fungal action and could originate the concentration of peloids (Figures 4C, 4D; Boggs Jr., 2006). This feature is typical of eodiagenesis (*i.e.*, shallow marine-phreatic diagenesis), indicating the first diagenetic phase and deposition in the photic zone at depths less than 200 m with partially or completely micritized grains (Tucker, 1992; Javanbakht *et al*., 2018; Khan *et al*., 2018; Sallam *et al*., 2019).

Neomorphism. In limestones, carbonate mud is the main constituent of lime-mudstones, wackstones, and packstones. However, this material is susceptible to change in size due to fluid action. This process occurs by recrystallization from mud to microcrystalline sparry calcite increasing the crystal size or dissolution and simultaneous precipitation of another minerals (Tucker, 1992; Flügel, 2004; Nichols, 2009). It is common in the microfacies Wb, Wbt, Pb, and Pbt where appears as a mass with different birefringence colors and crystal-sized. This process occurs in the meteoric diagenetic environment or the burial diagenetic environment, due to the dissolution of some crystals and the syntaxial growing of the another one showing lateral changes, whitish color, subhedral shapes and calcite composition (Figures 4E, 4F; Tucker and Wright, 1990). These reactions can be associated to the eodiagenesis in solid reactions evidenced for crystal-sized and calcite composition of matrix (Flügel, 2004; da Silva *et al*., 2015). The neomorphic crystals have the same composition of the micrite matrix.

Mechanical compaction. The progressive increase of sediment burial causes the physical compaction of carbonate constituents (Tucker, 1992; Valencia and Laya, 2020). This process starts during the eodiagenesis, and it is frequent in the microfacies Pb and Pbt which is indicated by deformed shapes and fractured bioclasts composed mainly by calcite (Figures 5A, 5B, 5C), reduction of the initial porosity of the rock, grain reorientation, packing, and dissolution (Boggs Jr., 2006; Ehrenberg and Baek, 2019). In the Sm facies, mechanical compaction is recognized by punctual and tangential contacts between quartz grains. In contrast, in the Fb microfacies, this compaction is recognized by the orientation of elongated bioclasts parallel to stratification.

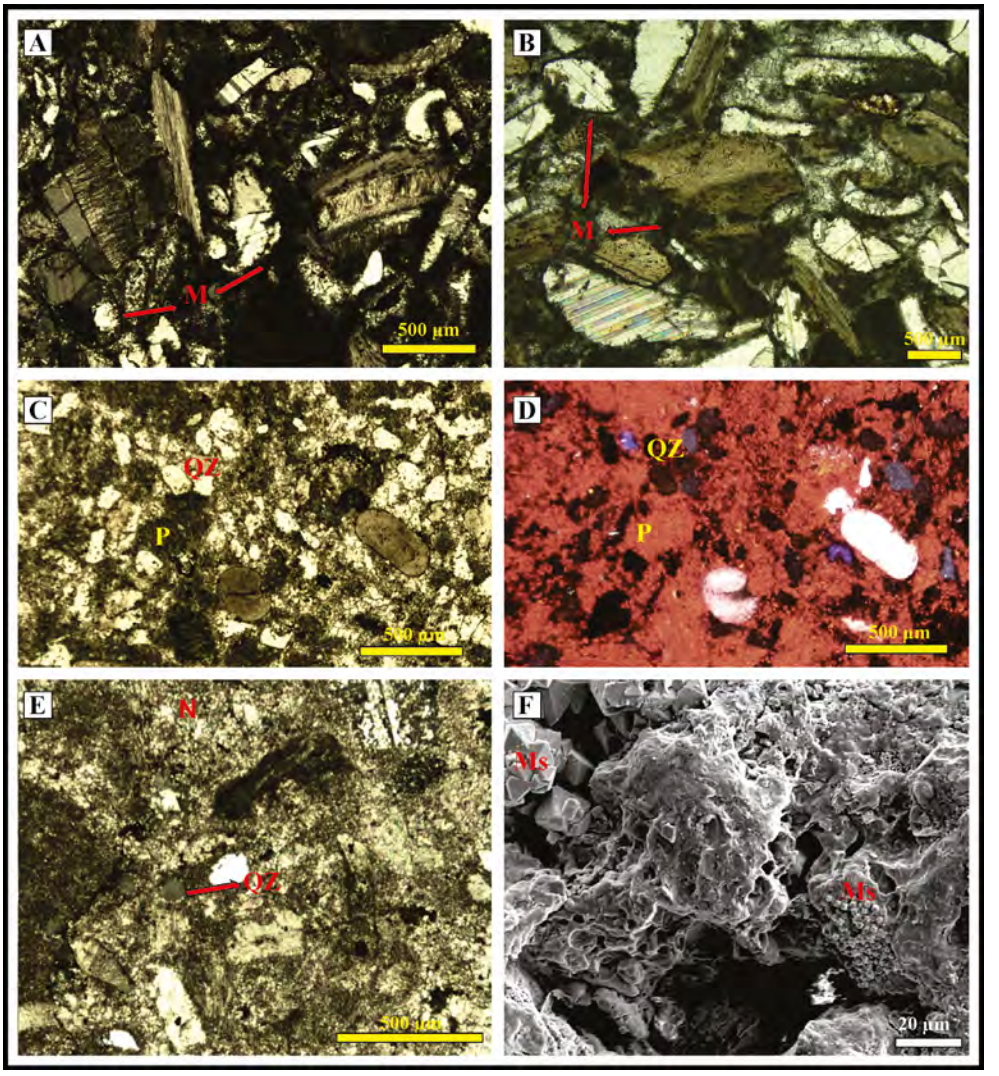

Figure 4. Micritization and neomorphism processes. **A.** and **B.** Microphotographs of fragmented bioclasts with dark envelopes and presence of micrite as sparry (matrix and cement). **C.** Image with the formation of peloids probably associated with micritization. **D.** CL image of C, showing spherical masses of calcite (red), quartz (gray), and clay minerals (blue). **E.** Microphotography with phases of recrystallization even formed pseudosparry. **F.** SEM image of secondary electrons showing the relation of two different sizes of microsparry. M: micrite envelopes, P: peloids, Qz: quartz, N: neomorphism, Ms: microsparry.

Cementation. Cementation consists of filling the porosity due to the action of saturated fluids (James and Coquette, 1990; Tucker, 1992; da Silva, 2019). The intensity of cementation in limestones depends mainly on the solute quantities from seawater as a result of the sedimentary processes like waves, tidal pumping, thermal convection, and diffusive transport (Boggs Jr., 2006). Commonly, most of the current carbonate cement characterized by high Mg calcite content. However, in ancient rocks, the composition exhibits generally low content of Mg calcite, which is concordant with limestones of Upper Tibasosa Formation (Scholle and Ulmer-Scholle, 2003). This phase occurs in all carbonate facies and microfacies filling vug pores, fractures, and bioclast. Their composition corresponds with calcite (Figures 5D, 5E, 5F), in different shapes such as equigranular, microcrystalline, bladed, and syntaxial (Figures 6B, 6C, 6D). The fluid action generates the partial dissolution of previous calcite crystals (Figure 6A), indicating an increase in the temperature.

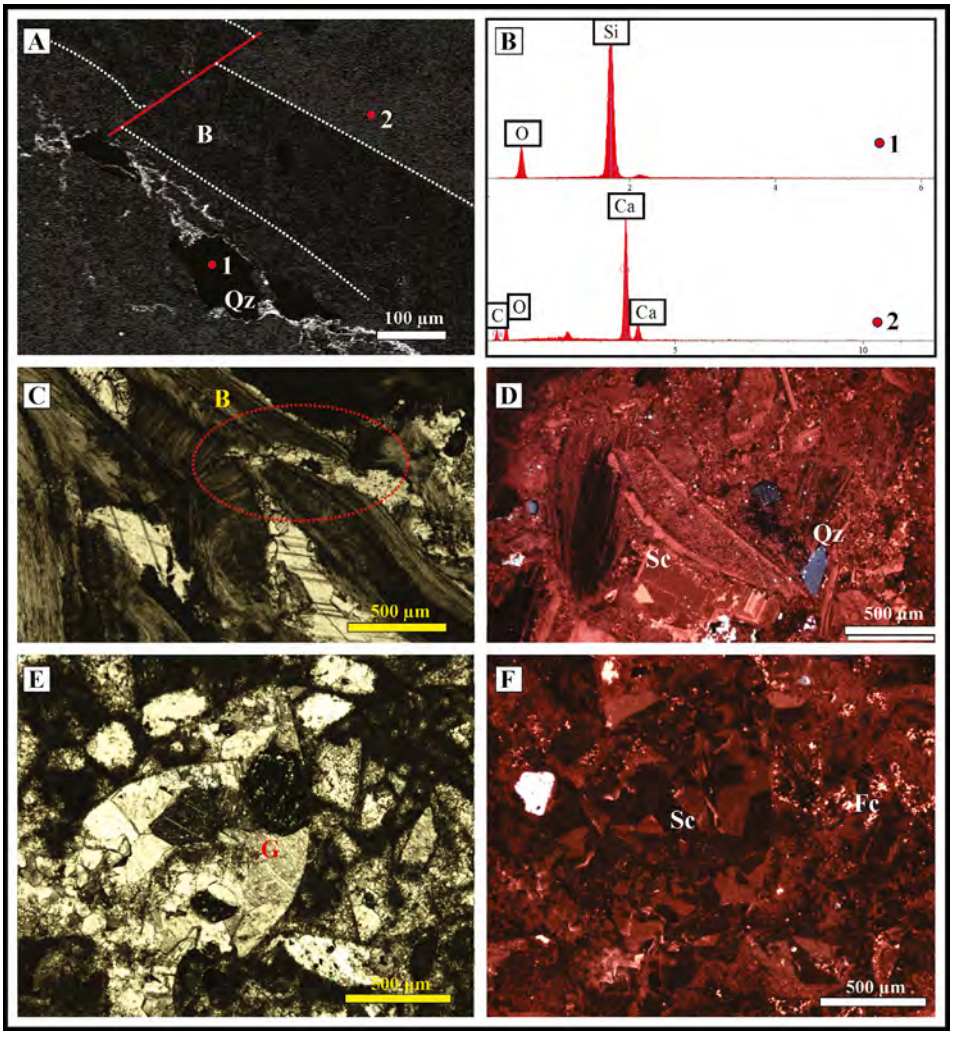

Figure 5. Mechanical compaction and cementation. **A.** SEM image of backscattering electrons (BSE) of a fragmented bioclast, the white line indicates the organism, and the red one shows a fracture and dislocation. **B.** Identification of quartz and calcite with EDS for points marked in A. **C.** Fragmented shell with percolation of sparry calcite (red circle). **D.** CL image showing the alternate of compositional bands in sparry calcite. **E.** Gastropod substituted by sparry calcite. **F.** CL image of E showing a compositional difference in sparry and a presence of fine calcite with a high content of Mn^{+2} (yellow luminescence). B: bioclast, Sc: sparry calcite, Qz: quartz, G: gastropod, Fc: fine calcite.

Cementation has at least four phases; the first generation is microcrystalline and corresponds to very fine crystals of calcite bordering the pores, generated during the meteoric phase. The second generation comprises equigranular calcite with medium size, subhedral shapes, clean aspect, and high interference color formed in the marine environment (Tucker, 1992; da Silva *et al*., 2015). The third generation consists of bladed calcite with wavy extinction formed in shallow marine zones evidencing overgrowths of non-luminescent (*e.g*., high Fe concentration) and luminescent bands (High Mg Calcite), due to the aragonite substitution and calcite precipitation (*e.g*., elevated Mn ions; Figures 6E, 6F; Flügel, 2004; Moore and Wade, 2013; Hiatt and Pufahl, 2014; Dickson, 2019). Finally, the fourth generation presents sparry calcite with coarse size, clean aspect, twinning, and sharp cleavage which is commonly substituting bioclasts, pores, and fractures (*i.e*., best developed in tectonized outcrops; Coniglio, 1989), it is formed by direct calcite precipitation and occasionally with differentiated compositional bands (Figure 5D). The Sm facies and Wbt/Pbt microfacies have an overgrowth of authigenic silica in quartz grains with poikilotopic calcite cement (Figure 3A).

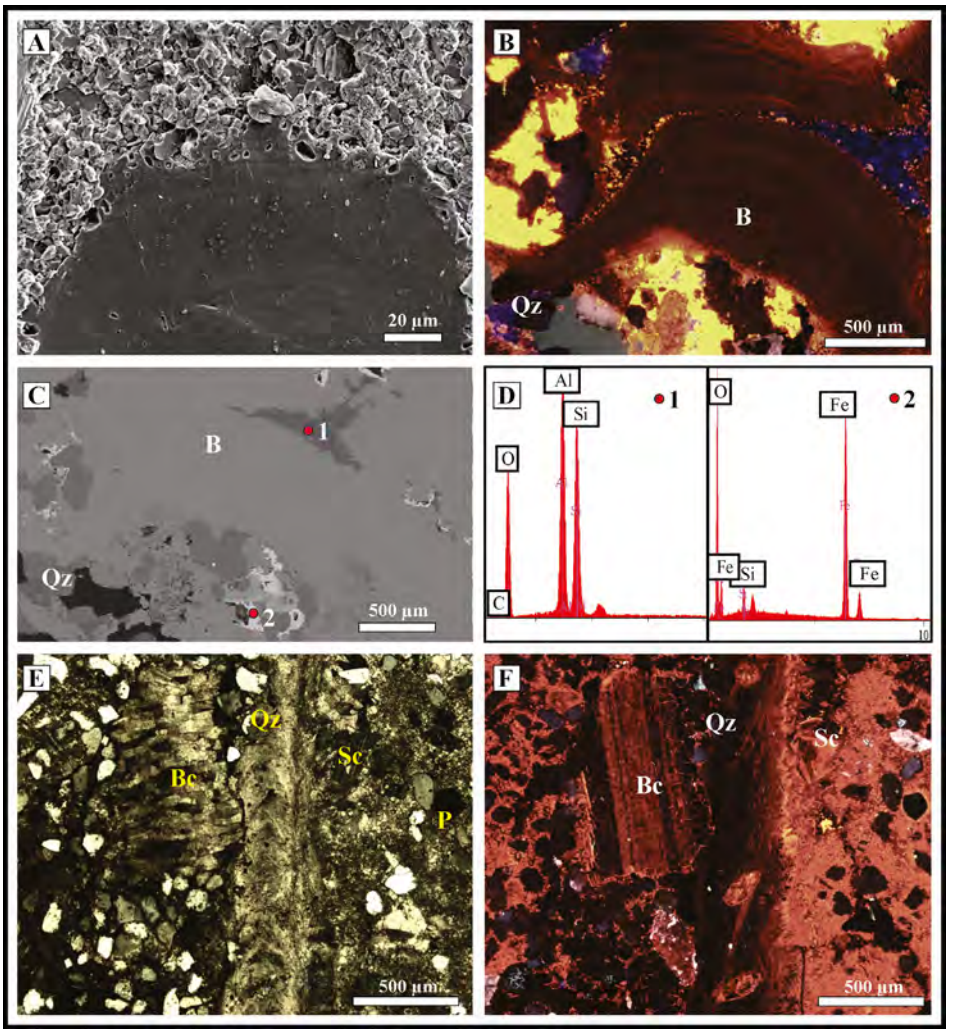

Figure 6. Cementation phases. **A.** SEM image of secondary electrons indicating the dissolution of carbonates. **B.** CL image showing carbonate cement with a high content of Mn^{+2} (yellow). **C.** SEM image of Backs Scattered Electron of B. **D.** EDS indicating clay minerals and iron oxides for points 1 and 2. **E.** Microphotography showing bladed calcite, quartz, and pyrite. **F.** CL image of E showing the compositional difference in bladed calcite and the presence of fine calcite with a high content of Mn^{+2} (yellow luminescence). Bc: bladed calcite, Sc: sparry calcite, Qz: quartz, P: pyrite, B: bioclast.

Chemical compaction. Chemical compaction and dissolution by pressure are burial processes associated with the solubility in the contact of grains and through sediment interfaces due to the tension gradient as the product of overburden charge and tectonics (Tucker and Wright, 1990). The carbonate dissolution allows the accumulation of insoluble (*e.g.*, often clay-rich) residues associated mainly to clay minerals, iron oxides/hydroxides and organic matter forming dissolution seams and stylolites (Figures 7A, 7B; Tada and Siever, 1989; Tucker and Wright, 1990; Toussaint *et al.*, 2018; da Silva, 2019). The evidence of mechanical and chemical compaction indicates mesodiagenetic processes, which may be accompanied by an increase of Mn^{2+}, Fe^{2+} (calcite), and silica cement (Scholle and Ulmer-Scholle, 2003). For this study were found mainly stylolites, dissolution seams, and embayed contacts, respectively.

Stylolites are rough dissolution surfaces displaying positive and negative peaks (teeth) of variable amplitudes (Bruna *et al.*, 2019), that form due to the intergranular pressure-solution resulting from burial compaction or tectonic stress (Humphrey *et al.*, 2019). They are formed by selective dissolution at a surface of the fabric and compositional change, mainly where exists tectonic activity, for the formation of this feature, are at least necessary about 300 m to 1000 m of burial supplying solutes for cementation (Scholle and Ulmer-Scholle, 2003), for this case are found mainly in the microfacies Pbt and Wbt. Dissolution seams

are present in isolated grains, especially between quartz and bioclastic fragments. Dissolved and sutures margins are recognized in bioclastic fragments (Figure 7A), these sutured contacts between grains could be an indication of extensive chemical compaction produced during burial diagenesis highlighted by the dark residues in the boundary of grains.

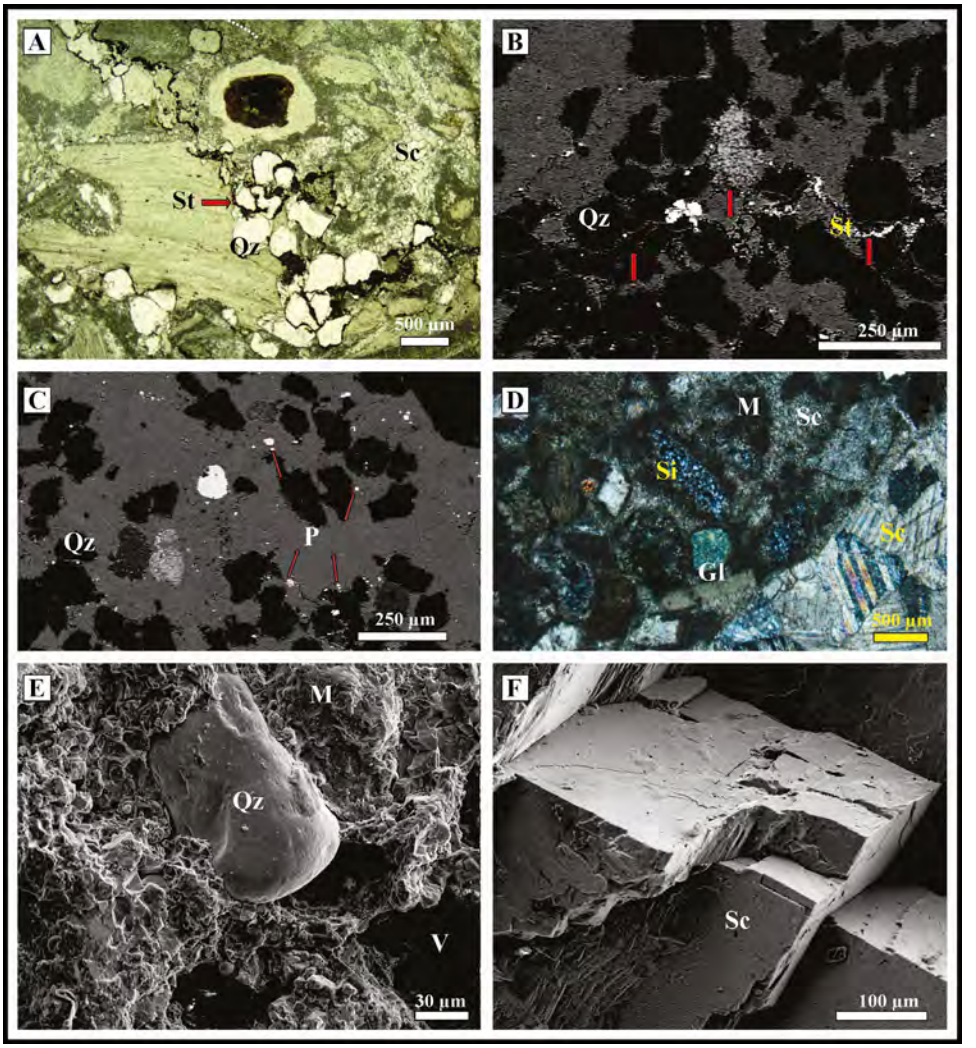

Figure 7. Chemical compaction, silicification, and porosity. **A.** Microphotography showing stylolites with the concentration of detrital quartz and iron oxides. **B.** SEM image of BSE with the concentration of clay minerals, iron oxides, and organic matter (red arrows indicate stylolites). **C.** SEM image of BSE with disseminated pyrite. **D.** Presence of silica in pores and bioclasts. **E.** SEM image of secondary electrons with vug pores. **F.** SEM image of secondary electrons evidencing sparry calcite filling fractures. St: stylolite, Si: silica, Gl: glauconite, M: micrite, V: vug pore, Sc: sparry calcite, Qz: quartz, P: pyrite.

Piritization. Pyrite corresponds with subhedral to framboidal shapes disseminated in the rock (Figure 7C), locally altered to iron oxides due to the subaerial exposure. This mineral formed in environments with a high content of organic matter and sulfides (*e.g.*, estuaries and tidal flats); in calcareous sediments, it is found next to detrital facies due to the iron ion availability (Berner, 1984). Localities with high rates of sulfide production by sulfate-reducing bacteria generate precipitation of monosulfides as greigite, which about 200°C could produce the formation of pyritic framboids (Wilkin and Barnes, 1997). However, its concentration is low because calcareous skeletal debris is poorer in iron than terrigenous grains (Berner, 1984; da Silva, 2019). Probably, the origin of iron is related to detrital transport because of it is found in microfacies with important terrigenous grains (Boggs Jr., 2006).

Silification. This process is frequent at the matrix and bioclasts in the microfacies Pb, Pbt, and Fb (Figure 7D), this silica consists of microcrystalline quartz indicating mesodiagenetic processes (Tucker, 1992). The authigenic silica in bioclasts formed as thin films on carapaces dissolving the carbonate and later precipitating (Maliva and Siever, 1988). The origin of that silica could be associated with quartz dissolution (Tucker and Wright, 1990; da Silva, 2019), supported because it is found mainly in carbonate rocks with a considerable content of terrigenous grains. In subaerial exposure silica replaced evaporites and generates chalcedony and chert beds (Shinn, 1983).

Porosity. Porosity in limestones of the Upper Tibasosa Formation is <5%, representing by vug, interparticle, intraparticle and moldic pores associated mainly with telodiagenetic processes owing to sample nature (from outcrops). The initial porosity probably reduced due to the lithostatic charge and cementation phases. In this case, different generations of calcite with coarser crystals in the middle filled vug pores (Choquette and Pray, 1970). The presence of porosity in this unit is low and probably is associated with the high content of matrix and cement, recognized in several microphotographs (Figure 7E). Fractures could increase permeability, reflecting burial diagenesis. However, most of the cases are filled with coarse calcite related to the migration of mineralizing fluids (Figure 7F). Moldic porosity represents telodiagenetic events (Scholle and Ulmer-Scholle, 2003; Moore and Wade, 2013).

Discussion

The Upper Tibasosa Formation offers the possibility for the study of carbonate platforms during the Lower Cretaceous; in this unit, the facies association allowed to determine the existence of two paleoenvironments: mixed tidal flats and a carbonate platform (Figure 8). The Tibasosa Formation recorded the incursion of the Cretaceous sea in the Eastern Cordillera Basin amplifying the tidal processes, which could be more evident in other stratigraphic sections and the correlated geological units in Colombia as the Paja, Ritoque, Rosablanca, Fomeque, Macanal, and Juntas formations (Reyes, 1984; Sarmiento-Rojas *et al.*, 2006; Miranda and Niño, 2016; da Silva, 2019).

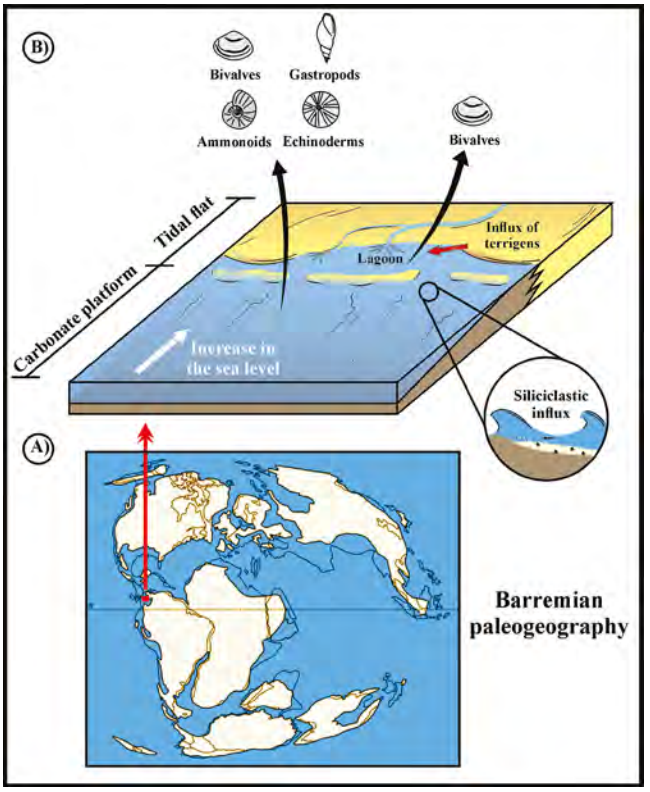

Figure 8. Paleoenvironmental interpretation for the Upper Tibasosa Formation. **A.** Barremian Paleogeography indicating the location of Colombia, modified of Smith *et al*. (1994) *apud* Patarroyo (2020). **B.** Facies associations for the Upper Member of the Tibasosa Formation.

The high content of fossils indicates the presence of shallow and warm waters, oxygenated environments, and Ph normal, allowing the conservation of carapaces of several organisms and subsequent reducing conditions during the burial phase according to the framboidal pyrite content (Wilkin and Barnes, 1997). The presence of a shell bed in the upper part of the outcrop could be a record of tsunamiites or tempestites (Figure 3B), being a possible explication of detrital quartz in the microfacies Wbt and Pbt (Puga-Bernabéu and Aguirre, 2017), however, its taphonomic attributes are not still understood completely, and it is necessary to study the areal disposition in other localities. The Lower Cretaceous carbonate platforms in Colombia characterized by abundance in the fossil content. The presence of ammonoids as *Niklesia* sp. as a key fossil allowed to delimit the studied stratigraphic section as Barremian deposits being coherent with the occurrence of other taxa as Echinoidea, Bivalvia and Gastropoda (Figure 9; Patarroyo, 2020). The paleogeographic distribution of the Paja, Ritoque, Rosablanca, Fomeque, Macanal, Juntas and the Upper Tibasosa formations provide tools to understand the lithologic changes associated with variations in bathymetry, sea-level rise, geological time, carbonate supply, and tectonics explaining why towards the west are frequent muddy siliciclastic rocks with abundant planktonic organisms while in the east exists more infaunal and epifaunal individuals (Patarroyo, 2020).

Figure 9. Main fossil groups for the Upper Tibasosa Formation. **A-D.** Gastropoda, **A-B**. *Neptunea* sp., **C-D.** *Tylostoma* sp., **E-J.** Bivalvia, **E-F.** *Pterotrigonia* sp., **G-H.** *Cardita* sp., **I-J.** *Ceratostreon* sp., **K-L.** Ammonoidea, **K-L.** *Nicklesia* sp., **M-P.** Echinoidea, **M-N.** *Nucleolites* sp., **O-P.** *Heteraster* sp. Scale 1 cm.

The occurrence of worldwide carbonate platforms during the Lower Cretaceous implies that variations in the eustatic sea-level controlled the deposition of marine sediments, representing an important transgressive surface as occurs in Asia (*e.g.*, Bachmann and Hirsch, 2006), Europe (*e.g.*, Hoedemaeker and Herngreen, 2003), Africa (*e.g.*, Reyment and Dingle, 1987), and America (*e.g.*, Barragán and Melinte, 2006; Patarroyo, 2020); recording similar depositional systems and fossil content to the Upper Tibasosa Formation.

The diagenetic sequence in carbonates of the Upper Tibasosa Formation indicates dominance of eodiagenetic processes such as micritization, neomorphism, physical compaction, porosity, dissolution, cementation (*e.g.*, microcrystalline, equigranular, bladed and sparry calcite) and pyritization; suggesting a primary marine origin of limestones (Figure 10). This kind of diagenesis occurs over short periods and involves a restricted range of fluid chemistry that explains the low variation of minerals (Scholle and Ulmer-Scholle, 2003). Likewise, the presence of bioclasts replaced by sparry calcite could be an indication of extensive dissolved bioclasts formed in the vadose zone during eodiagenesis that later were filled during the cementation phase. Commonly, the biological activity in the early stage of deposition affects the primary sedimentary structures and carbonates by boring, sediment ingestion, and low siliciclastic inflows; being the reason for the lack of sedimentary structures in these limestones during the biochemical precipitation. Also, mechanical compaction is responsible for bioclasts fragmentation, porosity reduction, and bed thinning altering the carbonate fabric in the early stages of diagenesis (Boggs Jr., 2006).

Mesodiagenesis recorded processes as chemical compaction and silicification. The generation of dissolution seams and stylolites can form early in burial depths less than 100 m (Toussaint *et al.*, 2018). However, stylolites in quartz mainly found at depths exceeding 1.5 km (Tada and Siever, 1989), explaining the presence of this feature in detrital quartz of limestones from the Upper Tibasosa Formation, concordant to the age and stratigraphic position of this unit in the Basin. High luminescence in CL could be associated with the relative high Mn/Fe ratio, which is frequent under reducing conditions during the early stage of burial diagenesis, also evidenced by the formation of framboidal pyrite at temperatures of about 200°C (Wilkin and Barnes, 1997; Cabral *et al.*, 2019). Formation of calcite with hard development of twinning, usually, involves dissolution and crystal dislocation as the result of burial loading or tectonic deformation (Figures 4B, 5C; Scholle and Ulmer-Scholle, 2003). The telodiagenetic events restricted to the iron oxides and hydroxides formation, moldic porosity, and evidence of chemical weathering in outcrops due to the dissolution of carbonates. The limestones presented disseminated iron filling pores and bioclasts, and it is frequent in altered pyrite preserving framboidal shapes after the uplift of the buried rocks owing to the tectonic influence during the Andean phase (Cooper *et al*., 1995). The most moldic pores recorded in macroscopic samples where there are molds of echinoderms and bivalves.

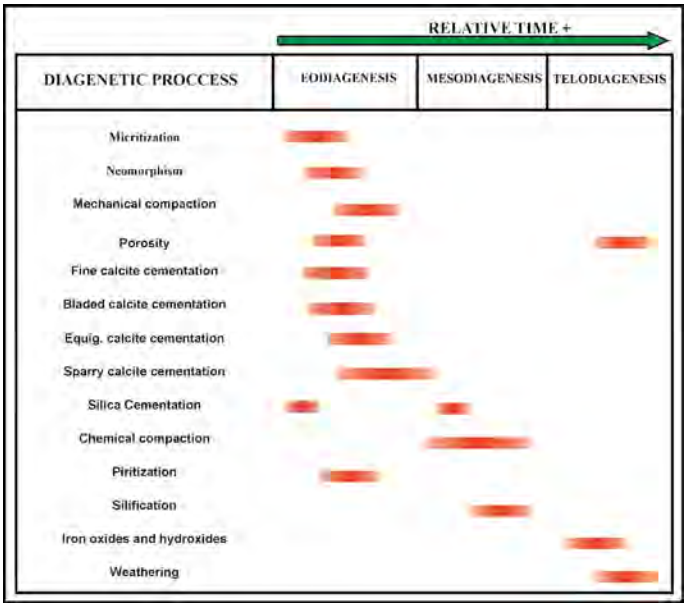

Figure 10. Scheme of diagenetic processes for the Upper Tibasosa Formation limestones with diagenetic environments (eodiagenesis, mesodiagenesis, and telodiagenesis).

Conclusions

The petrographic and faciological description allowed interpreting the possible environments of deposition for the Upper Tibasosa Formation, Firavitoba town in the Eastern Cordillera Basin. According to that, ten facies/microfacies grouped into two facies associations: mixed tidal flats (FA1) and carbonate platform (FA2). This sequence evidence a record of the Lower Cretaceous sea in the area of Sugamuxi Valley in Colombia. The presence of *Niclesia* sp., as key fossil and other genera association (*Neptunea*, *Tylostoma*, *Pterotrigonia*, *Ceratostreon*, *Nucleolites*, and *Heteraster*) allows positioning the outcrop in the Barremian Stage, as occurs in other localities in Asia, Europe, and Africa as a product of the eustatic sea-level increase in this time. Lithostratigraphic charts of the Middle Magdalena Valley, Eastern Cordillera, and Llanos basin indicate marine deposition for this age, in this way, shallow carbonate facies exhibit the presence of proximate continental facies represented by immature terrigenous grains which could be related to the Floresta paleo high.

Rocks of the Upper Tibasosa Formation exhibit the three major diagenetic phases: eodiagenesis, mesodiagenesis, and telodiagenesis. Micritization, dissolution, porosity, pyritization, neomorphism, cementation of calcite (*e.g.*, microcrystalline, equigranular, bladed, and sparry), and mechanical compaction; reflects the influence of eodiagenesis allowing to define a primary origin of these carbonate minerals and the low porosity. Chemical compaction, fracturing, and cementation of silica attributed to the mesodiagenesis due to the lithostatic charge and dissolution phases referred to burial processes. Iron oxides/hydroxides, weathering, and moldic porosity are related to the precipitation (*e.g.*, iron oxides) and dissolution of carbonates during the telodiagenesis. This work enables future correlations of the Upper Tibsasosa Formation with other carbonate platforms in the Lower Cretaceous in Colombia and around the World.

Acknowledgments

We thank the Research Group of Ingeniería Geológica of the Universidad Pedagógica y Tecnológica de Colombia (UPTC-Sogamoso) for the use of the petrography laboratory; the Research Group of Análise de Bacias sedimentares da Amazônia (GSED) for the discussion of this study, and the laboratories of Cathodoluminescence and Microanalysis in the Geoscience Institute of the Universidade Federal do Pará (Brazil).

References

Bachmann, M.; Hirsch, F. (2006). Lower Cretaceous carbonate platform of the eastern Levant (Galilee and the Golan Heights): stratigraphy and second-order sea-level change. *Cretaceous Research, 27*(4), 487-512. https://doi.org/10.1016/j.cretres.2005.09.003

Barragán, R.; Melinte, M.C. (2006). Palaeoenvironmental and palaeobiologic changes across the Barremian/Aptian boundary interval in the Tethys Realm, Mexico and Romania. *Cretaceous Research*, *27*(4), 529-541. https://doi.org/10.1016/j.cretres.2005.10.016

Berner, R.A. (1984). Sedimentary pyrite formation: an update. *Geochimica et Cosmochimica Acta*, *48*(4), 605-615. https://doi.org/10.1016/0016-7037(84)90089-9

Boggs Jr., S. (2006). *Principles of sedimentology and stratigraphy.* (4th ed.). Pearson Education, Inc.

Bruna, P.O.; Lavenu, A.P.C.; Matonti, C.; Bertotti, G. (2019). Are stylolites fluid-flow efficient features? *Journal of Structural Geology*, *125*, 270-277. https://doi.org/10.1016/j.jsg.2018.05.018

Cabral, F.A.A.; da Silveira, A.C.; Ramos, G.M.S.; de Miranda, T.S.; Barbosa, J.A.; Neumann, V.H.M.L. (2019). Microfacies and diagenetic evolution of the limestones of the upper part of the Crato Formation, Araripe Basin, northeastern Brazil. *Brazilian Journal of Geology*, *49*(1). https://doi.org/10.1590/2317-4889201920180097

Cediel, F. (1968). El grupo Girón, una molasa mesozoica de la Cordillera Oriental. *Boletín Geológico*, *16*(1-3), 5-96.

Choquette, P.W.; Pray, L.C. (1970). Geologic nomenclature and classification of porosity in sedimentary carbonates. *AAPG Bulletin, 54*(2), 207-250. https://doi.org/10.1306/5D25C98B-16C1-11D7-8645000102C1865D

Coniglio, M. (1989). Neomorphism and cementation in ancient deep-water limestones, Cow Head Group (Cambro-Ordovician), western Newfoundland, Canada. *Sedimentary Geology, 65*(1-2), 15-33. https://doi.org/10.1016/0037-0738(89)90003-1

Cooper, M.A.; Addison, F.T.; Alvarez, R.; Coral, M.; Graham, R.H.; Hayward, A.B.; Howe, S.; Martinez, J.; Naar, J.; Peñas, R.; Pulham, A.J.; Taborda, A. (1995). Basin development and tectonic history of the Llanos Basin, Eastern Cordillera, and Middle Magdalena Valley, Colombia. *AAPG Bulletin, 79*(10), 1421-1443.https://doi.org/10.1306/7834D9F4-1721-11D7-8645000102C1865D

da Silva, P.A.S. (2019). O mar epicontinental Itaituba na região central da Bacia do Amazonas: paleoambiente e correlação com os eventos paleoclimáticos e paleoceanográficos do carbonífero. Ph.D. Tese, Federal University of Pará, Belém, Pará, Brazil.

da Silva, P.A.S.; Afonso, J.W.L.; Soares, J.L.; Nogueira, A.C.R. (2015). Depósitos de plataforma mista, Neocarbonífero da bacia do Amazonas, região de Uruará, Estado do Pará. *Geologia USP, Série Científica*, *15*(2), 79-98. https://doi.org/10.11606/issn.2316-9095.v15i2p79-98

Dickson, J.A.D. (2019). Morphological analysis of archetypal calcite cement. *Journal of Sedimentary Research*, *89*(1), 66-87. https://doi.org/10.2110/jsr.2019.4

Dunham, R.J. (1962). Classification of carbonate rocks according to depositional texture. In: W. Ham (Ed.). *Classification of carbonate rocks* (pp. 108-121). Vol. 1, American Association of Petroleum Geologists Memoirs.

Ehrenberg, S.N.; Baek, H. (2019). Deposition, diagenesis and reservoir quality of an Oligocene reefal-margin limestone succession: Asmari Formation, United Arab Emirates. *Sedimentary Geology, 393-394*. https://doi.org/10.1016/j.sedgeo.2019.105535

Embry, A.F.; Klovan, J.E. (1971). A late Devonian reef tract on Northeastern Banks Island, NWT. *Bulletin of Canadian Petroleum Geology*, *19*(4), 730-781.

Flügel, E. (2004). *Microfacies of carbonate rocks. Analysis, interpretation, and application*. Springer-Verlag. Heidelberg.

Hiatt, E.E.; Pufahl, P.K. (2014). Cathodoluminescence petrography of carbonate rocks: application to understanding diagenesis, reservoir quality, and pore system evolution. In: I. Coulson (ed.). *Cathodoluminescence and its application to geoscience* (pp. 75-96). Vol. 45. Mineralogical Association of Canada, Short Course Series.

Hoedemaeker, P.J.; Herngreen, G.F.W. (2003). Correlation of Tethyan and Boreal Berriasian – Barremian strata with emphasis on strata in the subsurface of the Netherlands. *Cretaceous Research, 24*(3), 253-275. https://doi.org/10.1016/S0195-6671(03)00044-2

Humphrey, E.; Gomez-Rivas, E.; Koehn, D.; Bons, P.D.; Neilson, J.; Martín-Martín, J.D.; Schoenherr, J. (2019). Stylolite-controlled diagenesis of a mudstone carbonate reservoir: A case study from the Zechstein_2_Carbonate (Central European Basin, NW Germany). *Marine and Petroleum Geology, 109*, 88-107. https://doi.org/10.1016/j.marpetgeo.2019.05.040

James, N.P.; Coquette, P.W. (1990). Limestones: the sea floor diagenetic environment. In: I. Mcllrealth; D. Morrow (eds.). *Diagenesis* (pp. 13-34). Geoscience Canada.

Javanbakht, M.; Wanas, H.A.; Jafarian, A.; Shahsavan, N.; Sahraeyan, M. (2018). Carbonate diagenesis in the Barremian-Aptian Tirgan Formation (Kopet-Dagh Basin, NE Iran): Petrographic, geochemical and reservoir quality constraints. *Journal of African Earth Sciences, 144*, 122-135. https://doi.org/10.1016/j.jafrearsci.2018.04.016

Julivert, M. (1970). Cover and basement tectonics in the cordillera Oriental of Colombia, South America, and a comparison with some other folded chains. *GSA Bulletin, 81*(12), 3623-3646. https://doi.org/10.1130/0016-7606(1970)81[3623:CABTIT]2.0.CO;2

Khan, M.; Khan, M.A.; Shami, B.A.; Awais, M. (2018). Microfacies analysis and diagenetic fabric of the Lockhart Limestone exposed near Taxila, Margalla Hill Range, Punjab, Pakistan. *Arabian Journal of Geosciences, 11*(29). https://doi.org/10.1007/s12517-017-3367-4

Kiessling, W.; Flügel, E.; Golonka, J. (2003). Patterns of Phanerozoic carbonate platform sedimentation. *Lethaia*, *36*(3), 195-225. https://doi.org/10.1080/00241160310004648

Li, J.; Cai, Z.; Chen, H.; Cong, F.; Wang, L.; Wei, Q.; Luo, Y. (2018). Influence of differential diagenesis on primary depositional signals in limestone-marl alternations: an example from Middle Permian marine successions, South China. *Palaeogeography, Palaeoclimatology, Palaeoecology, 495*, 139-151. https://doi.org/10.1016/j.palaeo.2018.01.002

Maliva, R.G.; Siever, R. (1988). Mechanism and controls of silicification of fossils in limestones. *The Journal of Geology, 96*(4), 387-398. https://doi.org/10.1086/629235

Milliken, K. (2003). Diagenesis. In: G. Middleton (Ed.). *Encyclopedia of sediments* (pp. 214-219). Kluwer Academic Publishers.

Miranda, G.A.; Niño, C.M. (2016). Evaluación geológica, caracterización geomecánica y cálculo de recurso de roca caliza para el Contrato de Concesión Minera OG2-100 11 en la vereda Las Monjas del municipio de Firavitoba. Tesis, Universidad Pedagógica y Tecnológica de Colombia, Sogamoso, Colombia.

Moore, C.; Wade, W. (2013). *Carbonate reservoir: porosity and diagenesis in a sequence stratigraphic framework.* (2nd ed.). Elsevier.

Morad, S.; Suwaidi, M.A.; Mansurbeg, H.; Morad, D.; Ceriani, A.; Paganoni, M.; Al-Aasm, I. (2019). Diagenesis of a limestone reservoir (Lower Cretaceous), Abu Dhabi, United Arab Emirates: Comparison between the anticline crest and flanks. *Sedimentary Geology, 380,* 127-142. https://doi.org/10.1016/j.sedgeo.2018.12.004

Nichols, G. (2009). *Sedimentology and stratigraphy.* (2nd ed.). Wiley-Blackwell.

Patarroyo, P. (2002). Equinoideos del Miembro Calcáreo Superior, Formación Tibasosa, en el área de Firavitoba (Boyacá - Colombia). Morfología y fauna asociada. *Geología Colombiana, 27,* 95-107.

Patarroyo, P.; Rojas, A.; Salamanca, A. (2014). Stratigraphy of the Lower Calcareous Member (Valanginian - Hauterivian), Tibasosa Formation, Tibasosa – Boyacá (Colombia, S.A.). *23rd Latin American Colloquium on Earth Science,* Heidelberg, Germany.

Patarroyo, P. (2020). Barremian deposits of Colombia: A special emphasis on marine successions. In: J. Gómez; A.O. Pinilla-Pachon (eds.). *The Geology of Colombia* (pp. 445-474) Volume 2. Servicio Geológico Colombiano. https://doi.org/10.32685/pub.esp.36.2019.12

Pomar, L. (2001). Types of carbonate platforms: a genetic approach. *Basin Research, 13*(3), 313-334.

Puga-Bernabéu, A.; Aguirre, J. (2017). Contrasting storm- versus tsunami-related shell beds in shallow-water ramps. *Palaeogeography, Palaeoclimatology, Palaeoecology*, *471*, 1-14. https://doi.org/10.1016/j.palaeo.2017.01.033

Quintero, W.; Ladino, A.; Lozano, E.; Bolívar, O.; Zamora, N.; Rincón, J.; Puentes, M. (2014). Mapa de profundidad de la isoterma de Curie para Colombia. Bogotá: Servicio Geológico Colombiano.

Renzoni, G. (1981). Geología del cuadrángulo J-12 Tunja. *Boletín Geológico, 24*(2), 31-54.

Renzoni, G.; Rosas, H. (1967). Geología de la Plancha 171 Duitama. Ingeominas.

Renzoni, G.; Rosas, H.; Etayo, F. (1998). Geología Plancha 191 Tunja. Ingeominas.

Reyes, I. (1984). *Geología de la región Duitama-Sogamoso-Paz de Río (departamento de Boyacá)*. Universidad Pedagógica y Tecnológica de Colombia.

Reyment, R.A.; Dingle, R.V. (1987). Palaeogeography of Africa during the Cretaceous Period. *Palaeogeography, Palaeoclimatology, Palaeoecology*, *59*, 93-116. https://doi.org/10.1016/0031-0182(87)90076-9

Rojas, A.; Sandy, M.R. (2019). Early Cretaceous (Valanginian) brachiopods from the Rosablanca Formation, Colombia, South America: Biostratigraphic significance and paleogeographic implications. *Cretaceous Research, 96*, 184-195. https://doi.org/10.1016/j.cretres.2018.12.011

Sallam, E.S.; Afife, M.M.; Fares, M.; van Loon, A.J; Ruban, D.A. (2019). Sedimentary facies and diagenesis of the Lower Miocene Rudeis Formation (southwestern offshore margin of the Gulf of Suez, Egypt) and implications for its reservoir quality. *Marine Geology, 413*, 48-70. https://doi.org/10.1016/j.margeo.2019.04.004

Sarmiento-Rojas, L.F.; Van Wess, J.D.; Cloetingh, S. (2006). Mesozoic transtensional basin history of the Eastern Cordillera, Colombian Andes: Inferences from tectonic models. *Journal of South American Earth Sciences, 21*(4), 383-411. https://doi.org/10.1016/j.jsames.2006.07.003

Scholle, P.; Ulmer-Scholle, D. (2003). *A colour guide to the petrography of carbonate rocks: grains, textures, porosity, diagenesis*. American Association of petroleum geologists.

Seibel, M.J.; James, N.P. (2017). Diagenesis of Miocene, incised valley-filling limestones; Provence, Southern France. *Sedimentary Geology, 347,* 21-35. https://doi.org/10.1016/j.sedgeo.2016.09.006

Shinn, E.A. (1983). Tidal flats. In: P.A. Scholle; D.G. Bedout; C.H. Moore (eds.). *Carbonate depositional environments* (pp. 171-210). The American Association of Petroleum Geologists, Tulsa.

Smith, A.G.; Smith, D.G.; Funnell, B.M. (1994). *Atlas of Mesozoic and Cenozoic coastlines*. Cambridge University Press.

Tada, R.; Siever, R. (1989). Pressure solution during diagenesis. *Annual Review of Earth and Planetary Sciences, 17*, 89-118. https://doi.org/10.1146/annurev.ea.17.050189.000513

Toussaint, R.; Aharonov, E.; Koehn, D.; Gratier, J.P.; Ebner, M.; Baud, P.; Rolland, A.; Renard, F. (2018). Stylolites: a review. *Journal of Structural Geology, 114*, 163-195. https://doi.org/10.1016/j.jsg.2018.05.003

Tucker, M.E.; Wright, P. (1990). *Carbonate sedimentology*. Blackwell Scientific Publications.

Tucker, M.E. (1992). *Sedimentary petrology: an introduction*. (2nd ed.). Blackwell Scientific Publications.

Ulloa, C.E.; Guerra, A.; Escovar, R. (1998a). Geología de la Plancha 172 Paz de Río. Ingeominas.

Ulloa, C.E.; Rodríguez, E.; Escovar, R. (1998b). Geología de la plancha 192 Laguna de Tota. Ingeominas.

Valencia, F.L.; Laya, J.C. (2020). Deep-burial dissolution in an Oligocene-Miocene giant carbonate reservoir (Perla Limestone), Gulf of Venezuela Basin: Implications on microporosity development. *Marine and Petroleum Geology, 113*, 104-144. https://doi.org/10.1016/j.marpetgeo.2019.104144

Walker, R.G.; James, N.P. (1992). *Facies models reponse to sea level rise*. Geological Association of Canada L'Association giologique du Canada.

Wilkin, R.T.; Barnes, H.L. (1997). Formation processes of framboidal pyrite. *Geochimica et Cosmochimica Acta, 61*(2), 323-339. https://doi.org/10.1016/S0016-7037(96)00320-1

Received: 26 March 2020
Accepted: 01 October 2020